



ChemComm

**Robust Bis-rhodium(I) complex of  $\pi$ -extended planar, anti-aromatic hexaphyrin[1.0.1.0.1.0]**

Journal:	<i>ChemComm</i>
Manuscript ID	CC-COM-11-2019-009221.R1
Article Type:	Communication

SCHOLARONE™  
Manuscripts

## Robust Bis-rhodium(I) complex of $\pi$ -extended planar, anti-aromatic hexaphyrin[1.0.1.0.1.0]

Received 00th January 20xx,  
Accepted 00th January 20xx

Srinivas Samala,<sup>a</sup> Ranjan Dutta,<sup>a</sup> Qing He,<sup>b</sup> Yeonju Park,<sup>a</sup> Brijesh Chandra,<sup>a</sup> Vincent M. Lynch,<sup>c</sup> Young Mee Jung<sup>a</sup>, Jonathan L. Sessler<sup>\*,c</sup> and Chang Hee Lee<sup>\*,a</sup>

DOI: 10.1039/x0xx00000x

www.rsc.org/

**$\beta,\beta'$ -phenylene bridged hexaphyrin[1.0.1.0.1.0] (naphthosarin), an expanded porphyrin possessing C<sub>3v</sub>-symmetry, has been shown to possess unique electronic features. We now report a bimetallic Rh(I)-complex of naphthosarin retaining 24  $\pi$ -antiaromatic characteristics. The two Rh(I) cations reside on opposite sides of the macrocyclic  $\pi$ -system and are separated at a distance consistent with a possible Rh(I)-Rh(I) metallic bond interaction.**

Antiaromatic, expanded porphyrins are a unique class of porphyrin analogues<sup>1</sup> that often display interesting structural features and redox behaviour. Within this class,  $\beta,\beta'$ -phenylene bridged hexaphyrin[1.0.1.0.1.0] (naphthosarin; e.g., **2**, Figure 1) is of particular interest. It is a conformationally rigid 24  $\pi$ -electron system with *bona fide* antiaromatic character which exhibits proton-coupled electron transfer (PCET) upon protonation.<sup>2</sup> Prior investigations have served to confirm that the redox potential and electronic features are strongly influenced by the substituents and that by preparing appropriate derivatives. Such subtle structural modifications enabled stabilization of an one electron reduced form *i.e.* a 25  $\pi$ -electron radical species in the case of one particular naphthosarin.<sup>3</sup> However, in spite of this attention to the basic chemical features of naphthosarin, its metalation chemistry remains all but unexplored. In marked contrast, numerous metal complexes of other porphyrin analogues have been reported with a variety of metalation protocols suitable for use with *inter alia* porphyrins, corroles, carboxyporphyrins, N-confused porphyrins and numerous expanded porphyrins being known. The resulting metal complexes have been widely studied and have been successfully used in both catalytic<sup>4</sup> and biological applications.<sup>5</sup> In this context rhodium porphyrin complexes have

attracted considerable attention because of their unusual catalytic activity, including promoting selective C–H or C–C bond activation<sup>6</sup> as well as cycloadditions.<sup>7</sup> In the case of expanded porphyrins, both mono- and bis-rhodium complexes have been obtained depending on the size of the macrocyclic cavity and the number of nitrogen atoms present within the central core.<sup>8, 9,10-11</sup> This prior effort has provided us with an incentive to target for synthesis rhodium complexes of naphthosarin. Here, a key goal was to determine what effect, if any, metalation would have on this quintessential 24  $\pi$ -electron antiaromatic system.

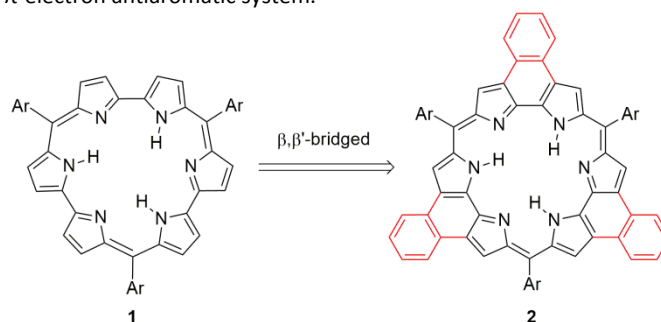


**Figure 1.** Chemical structures of hexaphyrin[1.0.1.0.1.0] (**1**) and  $\beta,\beta'$ -phenylene bridged hexaphyrin[1.0.1.0.1.0] (**2**).

To address this challenge, we elected to work with the *meso*-pentafluorophenyl  $\beta,\beta'$ -phenylene-bridged hexaphyrin[1.0.1.0.1.0] **2** (naphthosarin). From a structural point of view, this rosarin differs from the parent system **1** (Figure 1) in that it is conformationally rigid. Thus in **2** the  $\alpha,\alpha'$  positions are coplanar as revealed by prior structural studies.<sup>2</sup> As importantly, the 24-electron antiaromatic form is very stable in solution. In contrast, the corresponding two electron reduced, aromatic (26  $\pi$ -electron) form is unstable in solution. It undergoes rapid two-electron oxidation under ambient conditions to give the 24  $\pi$ -electron antiaromatic form. A <sup>1</sup>H NMR spectral analysis of this latter form revealed that the core N–H protons resonate at  $\delta$  26.02 ppm (in CDCl<sub>3</sub>). This chemical shift value presumably reflects an effective C<sub>3v</sub>-symmetry, a strong paratropic ring current effect with increased rigidity and, possibly,

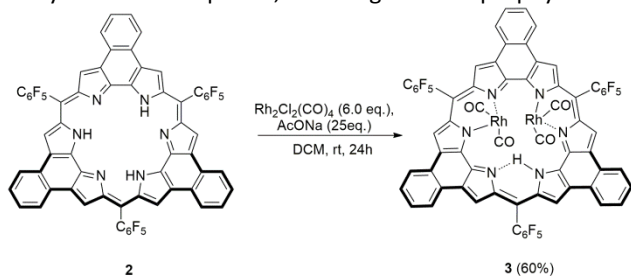
<sup>a</sup> Department of Chemistry, Kangwon National University, Chuncheon 24341, Korea.

<sup>b</sup> State Key Laboratory of Chemo/Biosensing and Chemometrics, College of Chemistry and Chemical Engineering, Hunan University, Changsha 410082, P. R. China

<sup>c</sup> Department of Chemistry, The University of Texas, Austin TX 78712-1224 USA. Electronic Supplementary Information (ESI) available: <sup>1</sup> NMR and CV data, ESI-MS data, crystallographic analysis of the compounds, characterization of the new compounds are available. See DOI: 10.1039/x0xx00000x

stronger intramolecular hydrogen bonding. In contrast, conversion of **2** to a rhodium complex was expected to lead to the loss of one or more of these core pyrrolic protons, resulting in changes that would be readily apparent in the  $^1\text{H}$  NMR spectrum.

As shown in Scheme 1, treatment of *meso*-pentafluorophenyl naphthosarin **2** with  $[\text{Rh}(\text{CO})_2\text{Cl}]_2$  in dichloromethane in the presence of excess sodium acetate afforded the bis-rhodium(I) complex **3** in 60% isolated yield.  $[\text{Rh}(\text{CO})_2\text{Cl}]_2$  is commercially available and is a standard reagent used in the synthesis of many rhodium complexes, including those of porphyrins.<sup>12</sup>



Scheme 1. Synthesis of Rh(I) complex **3**.

No other products could be isolated from the reaction mixture in appreciable quantities. Initial evidence that two rhodium centres were coordinated within the macrocyclic core came from MALDI-TOF mass spectrometric studies. For instance, a parent ion peak at  $m/z$  1349.981 (calcd  $m/z$  1349.954 for  $\text{C}_{63}\text{H}_{19}\text{F}_{15}\text{N}_6\text{Rh}_2$ ) was observed, as would be expected for complex **3**. A  $^1\text{H}$  NMR spectral analysis (Figure 2) provided support for the notion that complex **3** retains the antiaromatic character and paratropic ring current effects seen in **2**. For instance, one pyrrolic N–H resonance, appearing as a sharp singlet at 33.07 ppm, is observed. The downfield shift in this signal relative to the metal-free form **2** (26.02 ppm; see above) could reflect this proton existing in the form of an hydrogen bond bridge ( $\mu$ -hydrido) as inferred from the fact it proved non-exchangeable under standard  $\text{D}_2\text{O}$ -exchange conditions ( $\text{CD}_2\text{Cl}_2/\text{D}_2\text{O}$ ). Support for this contention came from a  $^1\text{H}$ – $^{15}\text{N}$  2D HSQC NMR experiment. As shown in Figure 3, a strong correlation was observed between the signals at 33 ppm ( $^1\text{H}$ ) and 282 ppm ( $^{15}\text{N}$ ). The chemical shift of  $^{15}\text{N}$  of complex **3** appeared at 282 ppm, which is significantly downfield shifted compared to that of aromatic porphyrins.<sup>13</sup>

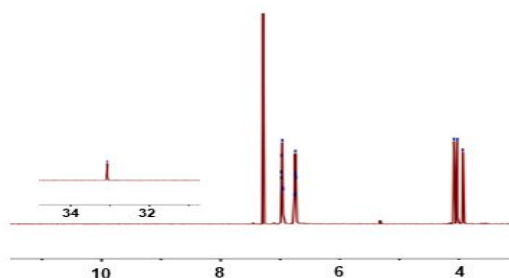


Figure 2.  $^1\text{H}$  NMR spectrum of the bis-rhodium complex **3** in  $\text{CDCl}_3$  (400 MHz) at 25 °C. The inset shows the inner pyrrole N–H resonance at  $\delta$  33.07 ppm.

The signals for the protons on the bridged phenylene group in compound **2** appear as two sets of doublets at 6.99 and 6.86

ppm in the  $^1\text{H}$  NMR spectrum, while the same protons appeared as multiplets ranging from 6.98 to 6.95 ppm in complex **3**. This increase in signal complexity is expected in light of the presumed  $\text{C}_{2v}$  symmetry of complex **3**. The indole protons in complex **3** appear as three sets of singlets at 4.08, 4.02, and 3.93 ppm, respectively. A  $^{13}\text{C}$  NMR spectral analysis of complex **3** revealed the presence of four carbonyl groups, as inferred from the observation of four distinct signals at 196.4, 195.8, 195.5, and 195.8 ppm, respectively (Figure S2, ESI). Furthermore, two strong absorption features, at 2010 and 2064  $\text{cm}^{-1}$ , ascribable to carbonyl stretching modes are seen in the IR spectrum of **3** (Figure S15, ESI).

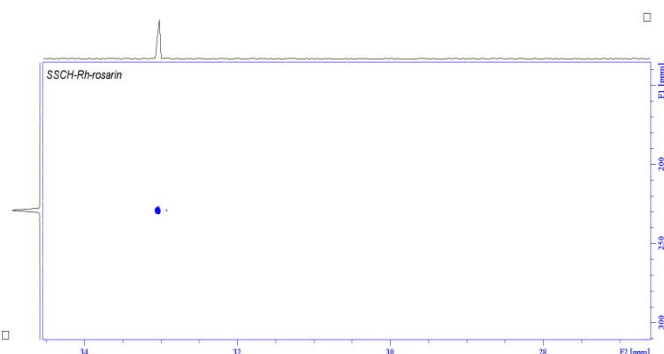


Figure 3. 850 MHz  $^1\text{H}$ – $^{15}\text{N}$  HSQC 2D NMR spectrum (partial) of complex **3** recorded in  $\text{CDCl}_3$  at 25 °C.

The solid state structure of complex **3** was determined unequivocally via a single-crystal X-ray diffraction analysis. Diffraction grade crystals of the complex **3** were obtained via the slow evaporation of solvent ( $\text{CHCl}_3$ ) at ambient temperature.

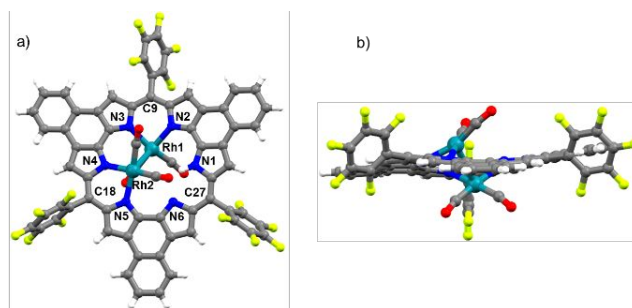
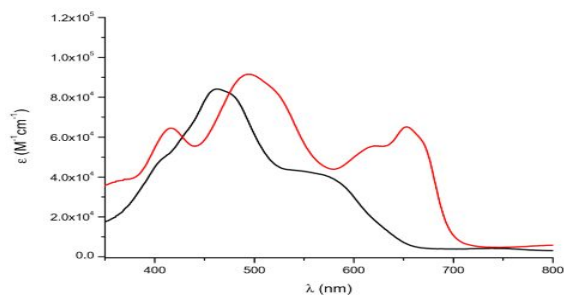


Figure 4. Single crystal X-ray diffraction analysis of complex **3**. ORTEP diagrams showing top (a) and side (b) views. The displacement ellipsoids have been scaled to the 50% probability level.

As shown in Figure 4, the ligand maintains its planarity but the two rhodium ions reside on opposite sides of the molecule resulting in inherent chirality. Two adjacent pyrrole nitrogen atoms (dipyrromethane-like) are bound to each Rh(I) centre with two carbonyl groups satisfying the coordination sphere giving rise to distorted square planar ligand geometry. The pyrrole nitrogen N–Rh distances are 2.119 Å (Rh1–N2), 2.128 Å (Rh1–N3), 2.164 Å (Rh2–N4), and 2.169 Å (Rh2–N5), respectively. Both rhodium centres lie outside the macrocyclic N6-plane (by 1.039 Å for Rh1 and 1.052 Å for Rh2). Similarly, Rh1 is located 0.136 Å out of the mean N2–N3–C1A–C2A plane, whereas Rh2 is

found to lie 0.098 Å out of the mean N4-N5-C3A-C4A plane. The intramolecular rhodium(I)-rhodium(I) distance (3.143 Å) could reflect the presence of a metallophilic interaction between the two Rh(I) ions.<sup>14</sup> The  $d^8$  electronic configuration and square planar geometry of Rh(I) ions also fulfil the criteria required for such a putative metallophilic interaction.<sup>15</sup>



**Figure 5.** UV-vis absorption spectra of the bis-Rh(I)-complex **3** (red) and free base **2** (black) in  $\text{CH}_2\text{Cl}_2$ .  $[\mathbf{3}] = [\mathbf{2}] = 6.83 \times 10^{-6} \text{ M}$ .

The UV-vis spectra of **2** and **3** are shown in Figure 5. The absorption spectrum of the bis-rhodium complex **3** was distinct from that of the free base **2**. In **3**, multiple absorption bands were observed between 416 nm and 496 nm, along with bands at 623 and 653 nm, respectively. In order to check the stability of complex **3** in the presence of acid and also to monitor its protonation behaviour, a UV-vis-spectral titration with trifluoroacetic acid (TFA) was performed in dichloromethane (ESI). The original absorption band appearing at 496 nm is shifted to 546 nm. This is most likely due to the formation of mono-protonated species. Notably, original absorption bands are fully recovered upon addition of triethylamine, leading us to conclude that complex **3** is stable in acid (Figure S17, ESI).

Since we previously demonstrated that the tri-protonated form of naphthosarin **2** can oxidize halide anions under proton coupled conditions to form one- or two-electron reduced species, the protonation behaviour of naphthosarin **2** and complex **3** were studied. Titrations with various acids, including HCl,  $\text{HClO}_4$ , MSA, and HI, were performed. A red-shifted absorption band at 546 nm was observed upon titration with  $\text{HClO}_4$  and MSA, which was ascribed to formation of a protonated form of complex **3** (S18, ESI). This protonated species is easily converted back to the original complex **3** upon treatment with TEA. However, different protonation features are observed upon titration with HCl and HI. For example, the addition of HCl to complex **3** resulted in gradual demetallation to give both naphthosarin **2** and a one-electron reduced 25  $\pi$ -electron dication radical form of the free base **2** (S19, ESI). Similar behaviour was observed upon addition of HI, but in this case the resulting 25  $\pi$ -electron species is further reduced to the corresponding 26  $\pi$ -electron aromatic species. This latter form is easily distinguished from other possible species due to the presence of a characteristic intense absorption band at 611 nm in its visible spectrum. Further treatment of the reduced 26  $\pi$ -electron aromatic species with DDQ serves to regenerate the free-base rosarin **2** (Figure S20, ESI).

The cyclic voltammogram (CV) of complex **3** recorded in  $\text{CH}_2\text{Cl}_2$  is shown in Figure 6. The CV of complex **3** mirror that recorded previously for the parent system (naphthosarin **2**), although with cathodic shifts in the oxidation and reduction waves. Two reduction potentials are seen in the CV of **3** at -1.18 and -0.69 V, whereas two reversible oxidation waves are observed at 0.25 and 0.68 V, respectively. An irreversible oxidation wave is also found at 1.05 V, which could reflect oxidation of the Rh(I) centre. The tendency to undergo reduction or oxidation seems less pronounced in the case of complex **3** than in the parent system **2**. As a consequence, reduction of compound **2** to the corresponding aromatic form becomes more difficult upon insertion of two rhodium(I) centres to produce complex **3**.

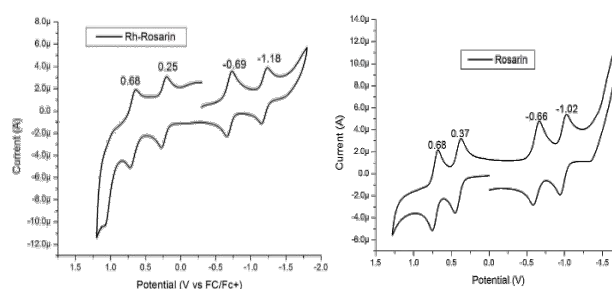


**Figure 6.** Cyclic voltammogram of complex **3** (left) and corresponding free base **2** ( $\text{Ar}=\text{C}_6\text{F}_5$ ), (right) measured at a scan rate of 100 mV/s in  $\text{CH}_2\text{Cl}_2$  using  $[\text{nBu}_4\text{N}][\text{PF}_6]$  (0.1 M) as the supporting electrolyte.

In summary, we have synthesized and characterized an antiaromatic binuclear Rh(I)-naphthosarin complex **3**. The synthesis was accomplished by the replacement of two inner core NH protons by Rh(I), which results in dramatic changes in the  $^1\text{H}$  NMR and UV-vis absorption spectra. A 2D  $^1\text{H}$ - $^{15}\text{N}$  HSQC spectral analysis serve to confirm that the downfield shifted N-H proton is involved in an intramolecular hydrogen bonding interaction with a neighbouring pyrrolic nitrogen atom, a finding that is thought to explain the lack of facile exchange in the presence of  $\text{D}_2\text{O}$ . A single crystal X-ray diffraction analysis revealed that the two rhodium(I) centres reside above and below the mean macrocyclic plane. The bound rhodium(I) centres are coordinated by two rosarin-derived nitrogen atoms and two ancillary CO ligands and exist in a distorted square planar geometry. The bis-rhodium complex **3** is protonated in the presence of TFA but is otherwise stable. A CV study revealed that reducing and oxidizing power of the complex **3** is reduced compared to that of the starting free base naphthosarin **2**. The present study thus reveals a manner whereby the fundamental properties of antiaromatic expanded porphyrins, such as rosarin, may be fine-tuned.

## Conflicts of interest

There are no conflicts to declare

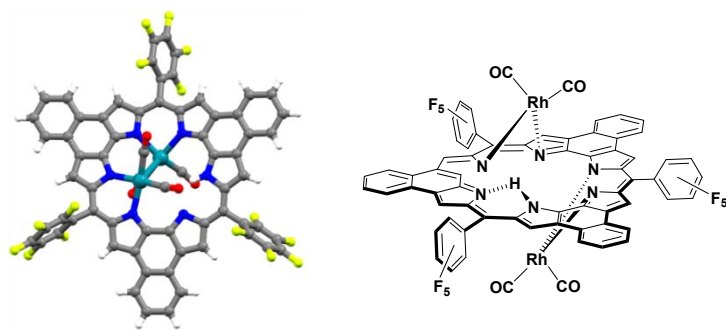
## Acknowledgements

Support is acknowledged from the Basic Science Research Program (NRF-2018R1A2A1A05077540) funded by the National Research Foundation under the Ministry of Science, ICT & Future Planning of Korea. The Central Laboratory at KNU is also acknowledged. The work in Austin was supported by the US National Science Foundation (CHE-1807152) and the Robert A. Welch Foundation F-0018).

## Notes and references

- (a) J.-Y. Shin, K. S. Kim, M.-C. Yoon, J. M. Lim, Z. S. Yoon, A. Osuka and D. Kim, *Chem. Soc. Rev.*, 2010, **39**, 2751; (b) J. Mack, *Chem. Rev.*, 2016, **117**, 3444; (c) B. K. Reddy, A. Basavarajappa, M. D. Ambhore and V. G. Anand, *Chem. Rev.*, 2017, **117**, 3420; (d) T. Tanaka and A. Osuka, *Chem. Rev.*, 2017, **117**, 2584; (e) R. R. Valiev, H. Fliegl and D. Sundholm, *Phys. Chem. Chem. Phys.*, 2017, **19**, 25979.
- M. Ishida, S.-J. Kim, C. Preihls, K. Ohkubo, J. M. Lim, B. S. Lee, J. S. Park, V. M. Lynch, V. V. Roznyatovskiy, T. Sarma, P. K. Panda, C.-H. Lee, S. Fukuzumi, D. Kim and J. L. Sessler, *Nat. Chem.*, 2012, **5**, 15.
- D. Firmansyah, S.-J. Hong, R. Dutta, Q. He, J. Bae, H. Jo, H. Kim, K.-M. Ok, V. M. Lynch, H.-R. Byon, J. L. Sessler and C.-H. Lee, *Chem. Eur. J.*, 2019, **25**, 3525.
- (a) E. B. Fleischer, *Acc. Chem. Res.*, 1970, **3**, 105; R. A. Sheldon, *Metalloporphyrins in Catalytic Oxidations*, Taylor & Francis, 1994; (b) K. M. Kadish, K. M. Smith and R. Guilard, *The Porphyrin Handbook: Applications: Past, Present, and Future*, Academic Press, 1999; (c) R. Bonnett, *Chem. Soc. Rev.*, 1995, **24**, 19; (d) Christopher J. Ziegler, *Studies into the Metal Chemistry of the Carbaporphyrinoids*, 2009.
- (a) K. M. Smith, *Porphyrins and Metalloporphyrins: A New Edition Based on the Original Volume by J. E. Falk*, Elsevier, 1975; (b) M. R. Wasielewski, *Chem. Rev.*, 1992, **92**, 435.
- (a) B. B. Wayland, S. Ba and A. E. Sherry, *J. Am. Chem. Soc.*, 1991, **113**, 5305; (b) Y. Aoyama, T. Yoshida, K.-I. Sakurai and H. Ogoshi, *J. Chem. Soc., Chem. Commun.*, 1983, 478; (c) X.-X. Zhang and B. B. Wayland, *J. Am. Chem. Soc.*, 1994, **116**, 7897; (d) W. Yang, H. Zhang, L. Li, C. M. Tam, S. Feng, K. L. Wong, W. Y. Lai, S. H. Ng, C. Chen and K. S. Chan, *Organometallics*, 2016, **35**, 3295; (e) K. S. Choi, P. F. Chiu and K. S. Chan, *Organometallics*, 2010, **29**, 624.
- (a) P. Tagliatesta, B. Floris, P. Galloni, A. Leoni and G. D'Arcangelo, *Inorg. Chem.*, 2003, **42**, 7701; (b) E. Elakkari, B. Floris, P. Galloni and P. Tagliatesta, *Eur. J. Inorg. Chem.*, 2005, 889; (c) P. Tagliatesta, E. Elakkari, A. Leoni, A. Lembo and D. Cicero, *New J. Chem.*, 2008, **32**, 1847; (d) M. Hasegawa, T. Kurahashi and S. Matsubara, *Chem. Lett.*, 2014, **43**, 1937.
- (a) H. Ogoshi, J. Setsune, T. Omura and Z. Yoshida, *J. Am. Chem. Soc.*, 1975, **97**, 6461; (b) D. Lexa, V. Grass and J.-M. Saveant, *Organometallics*, 1998, **17**, 2673; (c) W. Yang, H. Zuo, W. Y. Lai, S. Feng, Y. S. Pang, K. E. Hung, C. Y. Yu, Y. F. Lau, H. Y. Tsoi and K. S. Chan, *Organometallics*, 2015, **34**, 4051.
- (a) B. B. Wayland, B. A. Woods and V. M. Minda, *J. Chem. Soc., Chem. Commun.*, 1982, 634; (b) S. L. Van Voorhees and B. B. Wayland, *Organometallics*, 1985, **4**, 1887; (c) X. Fu, L. Basickes and B. B. Wayland, *Chem. Commun.*, 2003, 520; (d) S. J. Thompson, M. R. Brennan, S. Y. Lee and G. Dong, *Chem. Soc. Rev.*, 2018, **47**, 929.
- L. Yun, Z. Wang and X. Fu, *Inorg. Chem. Front.*, 2014, **1**, 544.
- I. Ogoshi, J.-I. Setsune, Y. Nanbo and Z.-I. Yoshida, *J. Organomet. Chem.*, 1978, **159**, 329; X. Liu, L. Liu, Z. Wang and X. Fu, *Chem. Commun.*, 2015, 51, 11896.
- (a) E. B. Fleischer and N. Sadasivan, *Chem. Commun.*, 1967, 159; (b) M. Toganoh, T. Niino, H. Maeda, B. Andrioletti and H. Furuta, *Inorg. Chem.*, 2006, **45**, 10428; (c) Q.-C. Chen, I. Saltsman, A. Kaushansky, Z.-Y. Xiao, N. Fridman, X. Zhan, and Z. Gross, *Chem. Eur. J.*, 2018, **24**, 17255; (d) T. D. Lash, W. T. Darrow, A. N. Latham, N. Sahota, and G. M. Ferrence, *Inorganic Chemistry*, 2019, **58**, 7511.
- D. Gust and J. D. Roberts, *J. Am. Chem. Soc.*, 1977, **99**, 3637.
- (a) M. Jakonen, L. Oresmaa and M. Haukka, *Crystal Growth & Design*, 2007, **7**, 2620; (b) E. Laurila, R. Tatikonda, L. Oresmaa, P. Hirvaa and Matti Haukka, *CrystEngComm*, 2012, **14**, 8401; (c) N. A. Bailey, E. Coate, G. B. Robertson, F. Bonati, R. Ugo, *J. Chem. Soc., Chem. Commun.*, 1967, 1041.
- L. H. Doerr, *Dalton Trans.*, 2010, **39**, 3543.

## Graphical Abstract



**A bimetallic Rh(I)-complex of a 24  $\pi$ -electron hexaphyrin with intrinsic antiaromaticity is reported.**